Published in final edited form as:
J Am Coll Cardiol. 2014 January 7; 63(1): 40–48. doi:10.1016/j.jacc.2013.07.098.

Multistage Electrotherapy Delivered Through Chronically-Implanted Leads Terminates Atrial Fibrillation With Lower Energy Than a Single Biphasic Shock

Ajit H. Janardhan, MD, PhD[*], **Sarah R. Gutbrod, MS**[†], **Wenwen Li, PhD**[†], **Di Lang, PhD**[†], **Richard B. Schuessler, PhD**[†,‡], and **Igor R. Efimov, PhD**[*,†]

[*]Department of Medicine, Cardiovascular Division, Washington University School of Medicine, St. Louis, Missouri

[†]Department of Biomedical Engineering, Washington University, St. Louis, Missouri

[‡]Department of Surgery, Cardiothoracic Division, Washington University School of Medicine, St. Louis, Missouri

Abstract

Objectives—The goal of this study was to develop a low-energy, implantable device–based multistage electrotherapy (MSE) to terminate atrial fibrillation (AF).

Background—Previous attempts to perform cardioversion of AF by using an implantable device were limited by the pain caused by use of a high-energy single biphasic shock (BPS).

Methods—Transvenous leads were implanted into the right atrium (RA), coronary sinus, and left pulmonary artery of 14 dogs. Self-sustaining AF was induced by 6 ± 2 weeks of high-rate RA pacing. Atrial defibrillation thresholds of standard versus experimental electrotherapies were measured in vivo and studied by using optical imaging in vitro.

Results—The mean AF cycle length (CL) in vivo was 112 ± 21 ms (534 beats/min). The impedances of the RA–left pulmonary artery and RA–coronary sinus shock vectors were similar (121 ± 11 Ω vs. 126 ± 9 Ω; $p = 0.27$). BPS required 1.48 ± 0.91 J (165 ± 34 V) to terminate AF. In contrast, MSE terminated AF with significantly less energy (0.16 ± 0.16 J; $p < 0.001$) and significantly lower peak voltage (31.1 ± 19.3 V; $p < 0.001$). In vitro optical imaging studies found that AF was maintained by localized foci originating from pulmonary vein–left atrium interfaces. MSE Stage 1 shocks temporarily disrupted localized foci; MSE Stage 2 entrainment shocks continued to silence the localized foci driving AF; and MSE Stage 3 pacing stimuli enabled consistent RA–left atrium activation until sinus rhythm was restored.

Conclusions—Low-energy MSE significantly reduced the atrial defibrillation thresholds compared with BPS in a canine model of AF. MSE may enable painless, device-based AF therapy.

Reprint requests and correspondence: Dr. Igor R. Efimov, Biomedical Engineering Department, Washington University, 1 Brookings Drive, St. Louis, Missouri 63130. igor@wustl.edu.

Keywords

atrial fibrillation; cardioversion; defibrillation; low energy; multistage electrotherapy

Atrial fibrillation (AF) is the most common tachyarrhythmia worldwide, and the number of Americans afflicted with AF is projected to reach 12 million by 2050 (1). Although catheter ablation has become increasingly common for the treatment of AF, it imposes a significant risk of complications, and recurrence after a single catheter ablation procedure is relatively high (2). Cardioversion of AF by using high-voltage external biphasic shocks remains a mainstay of therapy. However, external cardioversion incurs costly anesthesia and hospitalization expenses; treatment fees associated with AF are estimated to cost Medicare more than $15.7 billion annually (3).

Internal atrial cardioversion requires significantly less energy than external cardioversion (4). Thus, it may be possible to cardiovert AF internally below the pain threshold, which is variably reported to be between 0.1 J and 1 J (5,6). These considerations prompted efforts to design an implantable device that converts AF to sinus rhythm safely and painlessly, thereby ameliorating symptoms and potentially reducing the likelihood of atrial remodeling (7). Historically, these attempts failed largely due to the fact that the atrial defibrillation threshold (DFT) of a single biphasic shock (BPS) remains above the pain threshold (8-11).

We, therefore, developed an electrotherapy protocol arising from the demonstrated phase dependence of the tissue response to shocks (12). This therapy was developed from the initial discovery that there is a shock strength phase dependence for successful unpinning of atrial and ventricular tachyarrhythmias (13,14) and the notion that multiple pulses increase the probability of delivering a low-voltage shock during the optimal temporal window (12,15). From these initial studies, we hypothesized that a further decrease in peak voltage could be achieved if the multiple pulses were followed by antirepinning phases to prevent the reinitiation of AF. We previously tested several stages of multistage electrotherapy (MSE) and found that the 3-stage therapy resulted in the lowest atrial DFT (16). Therefore, our novel electrotherapy consists of 3 stages of successively decreasing energy levels, which we refer to as MSE (16,17). In the present study, we prospectively compared MSE with BPS to establish the defibrillation threshold in a canine in vivo model of tachypacing-induced AF, delivered through chronically-implanted transvenous leads. Subsequently, we investigated the mechanism by which MSE terminates AF by using optical mapping.

Methods

Surgical procedures

All animal procedures were performed in accordance with the position of the American Heart Association on the use of research animals (updated in 1985) and were approved by the Washington University Animal Studies Committee. Mongrel dogs (N = 14) weighing 20 to 25 kg were anesthetized, and pacing/defibrillation leads (Medtronic, Inc., Minneapolis, Minnesota) were introduced from the right internal jugular vein with fluoroscopic guidance. In all dogs, a pacing lead (model number 5096; Medtronic, Inc.) was implanted into the right

atrial appendage (RAA), and defibrillation leads were implanted into the RAA (model number 6935; Medtronic, Inc.), left pulmonary artery (LPA), and coronary sinus (CS) (model number 6937A; Medtronic, Inc.). The CS of canine hearts often tapers abruptly, preventing implantation of a lead in the distal CS. The inferior branch of the LPA runs adjacent to the lateral CS and was therefore used to anatomically approximate the clinical distal CS implantation site (Fig. 1A).

The pacing lead was connected to an implanted high-rate pacing (HRP) device (Medtronic, Inc.) programmed with custom software. Defibrillation leads were connected to custom subcutaneous access ports (Evergreen Medical Technologies, Minneapolis, Minnesota). Figure 1 shows fluoroscopic and schematic images depicting subcutaneous access ports and lead positions.

Each animal underwent a complex experimental protocol, including the surgical implant and subsequent defibrillation studies. A timeline illustrating the experimental sequence of events is shown in Figure 1C.

During survival defibrillation studies, animals were reanesthetized, and the subcutaneous access ports were accessed transcutaneously by using needle electrodes (Evergreen Medical Technologies) under fluoroscopic guidance. Blood pressure, electrolyte levels, and arterial oxygen saturation were monitored continuously.

HRP-induced self-sustaining AF

The HRP at 400 beats/min began 1 week after implantation from the RAA pacing lead at twice the atrial capture threshold. Digoxin (Jerome Stevens Pharmaceuticals, Inc., Bohemia, New York) was administered orally once daily to limit the ventricular rate during HRP and AF. Device and rhythm checks were performed weekly to determine AF induction. AF was defined as an irregular fast atrial rhythm occurring at a cycle length (CL) of <150 ms (>400 beats/min). For this study, AF was defined as self-sustained AF lasting >30 min during interrogation. Once this arrhythmia was observed, the animal was rechecked 1 week later to determine if AF persisted for ≥1 week. If AF was present, survival defibrillation studies were performed. After the final in vivo defibrillation study, hearts were explanted for the in vitro mechanism investigations.

Atrial and ventricular shock excitation thresholds

Animals in AF at the start of the defibrillation study underwent cardioversion by using a 10- to 30-J external shock to enable accurate measurement of the atrial shock excitation threshold (ASET) and the ventricular shock excitation threshold (VSET) during sinus rhythm. ASET and VSET, defined as the minimum energy by which a 10-ms monophasic square wave shock excited the atrium or ventricle, respectively, were measured for each defibrillation vector (RA-CS and RA-LPA) at the start of each in vivo defibrillation study during the diastolic interval during sinus rhythm. Shock excitation thresholds were determined by evaluation of surface and endocardial electrograms.

Electrotherapies tested

The electrotherapies tested are shown in Figure 2A. BPS (Fig. 2A, left panel) triggered to the ventricular R-wave (6/4 ms duration and a 2:1 ratio of the leading-edge voltages of the 2 phases) was compared with MSE (Fig. 2A, right panel). Before each application of MSE, AF was analyzed using a fast Fourier transform algorithm to determine the dominant frequency, which was expressed as a CL. Once the AF CL was determined, the MSE was delivered in 3 stages. In Stage 1, 2 biphasic shocks (6/4 ms duration and 2:1 ratio of the leading-edge voltages of the 2 phases) were delivered within 1 length of the AF CL (time between the 2 shocks was equal to 50% of AF CL) and were triggered to the R-wave. After a 50-ms delay, Stage 2 of MSE was delivered and consisted of 6 monophasic shocks (each 10 ms in duration) delivered at an interval of 88% of the AF CL and at a voltage that is 60% of the VSET. After another 50-ms delay, Stage 3 of MSE was delivered; it consisted of pacing from the RAA lead at an interval of 88% of the AF CL, delivered at twice the atrial pacing threshold. Importantly, the only change in MSE after an unsuccessful cardioversion was an increase in the Stage 1 peak leading-edge voltage (i.e., the peak voltage of the 2 biphasic shocks delivered within a single AF CL). Stage 2 shocks were fixed for each animal based on VSET, whereas Stage 3 pacing remained fixed for a given animal based on the atrial pacing capture threshold; once established at the outset of the in vivo cardioversion studies, Stage 2 and 3 amplitudes did not vary.

Similarly, the only change to the BPS electrotherapy after an unsuccessful cardioversion was an increase in the peak leading-edge voltage.

Defibrillation protocol for in vivo survival studies

AF was induced by 50-Hz burst pacing from the RAA pacing lead at twice the atrial pacing threshold. The mean AF CL was determined for AF lasting >5 min by using a real-time fast Fourier transform algorithm. Atrial DFTs of both electrotherapies were measured by using a randomized, voltage-regulated, step-up protocol. After each induction of AF, either BPS or MSE was randomly chosen. Once chosen, the specified therapy was applied. For BPS, the peak leading-edge voltage was applied initially at twice the ASET and then doubled until successful cardioversion. For MSE, the peak leading-edge voltage of Stage 1 biphasic shocks was initially applied at twice the ASET and then followed by fixed voltages and pacing outputs for Stage 2 and Stage 3, respectively. After unsuccessful cardioversion by MSE, only the peak leading-edge voltage of Stage 1 (2 biphasic shocks) was doubled, and MSE was reapplied until successful cardioversion. Successful cardioversion was defined as the restoration of sinus rhythm within 10 s of the start of therapy application. To prevent time-dependent carryover effects on the measurement of atrial DFT, a 5-min rest period was observed after each successful cardioversion (16). Electrotherapies were delivered from computer-controlled, regulated power supplies (BOP 100-4M, Kepco, Inc., Flushing, New York). Impedances were calculated by using a current probe (A622, Tektronix, Inc., Beaverton, Oregon) during the shock excitation threshold testing shocks. At the conclusion of each survival defibrillation study, HRP was resumed after a 24-h recovery period.

Optical mapping of MSE in vitro

After the final defibrillation study, the heart was perfused in a retrograde fashion through the aorta with heparinized cardioplegic solution and explanted. Ventricles were removed, and the endocardial surfaces of the atria and pulmonary veins (PVs) were exposed. The right and left coronary arteries were perfused with oxygenated Tyrode's solution, Blebbistatin (R&D Systems, Ellisville, Missouri), to reduce motion artifact, and a fluorescent, voltage-sensitive dye (Di-4 ANEPPS, Molecular Probes, Eugene, Oregon) to enable recording of optical action potentials. Optical action potentials (OAPs) were acquired by using a CMOS camera (SciMedia USA Ltd., Costa Mesa, California) with high spatial (100 × 100 pixels) and temporal (1,000 frames/s) resolution from a 2.5 × 2.5 cm field of view. Two silver/silver chloride–sensing electrodes were placed lateral to the LA and RA for constant monitoring. A bipolar RAA electrode was used for pacing and induction of AF by 50-Hz burst pacing. Electrotherapies were delivered from 2 parallel mesh electrodes placed lateral to the LA and RA 10 cm apart. Optical mapping was performed as described previously (18). To capture the arrhythmia, application of therapy, and the immediate tissue response, 8-s optical files were recorded for each trial. The optical files were analyzed to determine the spatiotemporal characteristics of the induced arrhythmias. This method included the local dominant frequencies and the regularity index, which is a signal-processing measure of the stability of the periodicity of the arrhythmia at each location (19). It is calculated as the ratio of the power in a 1-Hz band centered on the dominant frequency compared with the total power across all frequencies up to 200 Hz. In addition, the sequential tissue response to each stage of therapy was analyzed by observing the advancement of the wave front. Both OAP and phase were used in this analysis, as previously described (20).

Statistical analysis

The defibrillation protocol randomized the sequence of electrotherapies to prevent the confounding effects of treatments with respect to time. Recovery periods were observed after each AF termination to prevent carryover effects. Paired Student *t* tests were used to compare ASET with VSET for a given shock, and the Mann-Whitney test was used to compare impedances of the 2 vectors by using Prism 5.0c (GraphPad Software, La Jolla, California). DFT comparisons were analyzed with a linear mixed random effects model with animal identification as a random effect and the period between treatments as a fixed effect. Animal identification × therapy was also analyzed as a random effect to test for interactions. Estimates were calculated with the MIXED procedure in SAS version 9.2 (SAS Institute, Inc., Cary, North Carolina). Results are reported as mean ± SD. A p value of ≤0.05 was considered significant.

Results

Chronic HRP model of AF

Of the 14 canines implanted, 4 were euthanized before DFT testing was performed due to systemic bacterial infection. The remaining 10 dogs developed self-sustained AF. Eight dogs were used for in vivo survival defibrillation studies and 7 were used for terminal optical mapping studies (5 canines were used for both studies). The mean duration of HRP required to induce self-sustaining AF was 6 ± 2 weeks. The mean AF CL in vivo was 112 ± 21 ms.

For the RA-LPA vector, the mean ASET was 4.1 ± 2.9 V, and the mean VSET was 8.1 ± 3.2 V ($p < 0.001$). For the RA-CS vector, the mean ASET was 3.3 ± 0.5 V, and the mean VSET was 8.0 ± 3.2 V ($p < 0.001$). The impedances of the RA-LPA and RA-CS vectors were not statistically different (121 ± 11 Ω vs. 126 ± 9 Ω, respectively; $p = 0.27$).

In vivo atrial cardioversion studies

A total of 32 in vivo defibrillation studies were performed in 8 dogs. A total of 123 episodes of sustained AF were successfully converted to sinus rhythm, yielding an average of 3.8 cardioversions per study. Sample terminations by BPS and MSE in a single survival defibrillation study are shown in Figure 2B. In this example, the atrial DFT of BPS was 170 V (1.65 J) compared with 2.5 V (0.02 J) for MSE. Average results (8 dogs) are shown in Figure 2C. The mean DFT of MSE was significantly lower compared with that of BPS in terms of total energy (0.16 ± 0.16 J vs. 1.48 ± 0.91 J, respectively; $p < 0.001$) and peak shock voltage (31.1 ± 19.3 V vs. 165 ± 34 V, respectively; $p < 0.001$). Importantly, these results demonstrate that atrial DFT can be effectively lowered by using commercially available transvenous implantable leads placed in RA and CS.

In vitro organization of AF

The hearts of 7 dogs with self-sustaining AF induced by HRP were explanted for mechanistic studies. Due to denervation, some hearts required the perfusion of acetylcholine to induce sustained AF in vitro. A representative in vitro AF episode is shown in Figure 3. The optical imaging field of view is shown in Figure 3A. Notably, this view incorporated the interfaces between the PVs and the left atrium (LA). Figure 3B illustrates the spatial relationship of the dominant frequencies across the field of view (frequency resolution of 0.25 Hz). Sample optical recordings are shown from the highest dominant frequency locations. Interestingly, the highest frequency components (in this heart) originated in the right and left superior PVs. High-frequency drivers of AF were seen at the PVs or LA-PV interfaces in all canine hearts imaged in vitro (data not shown). Figure 3C shows an analysis of the regularity index; the highest and most stable frequencies were located at the PV or PV-LA interfaces. Taken together, these observations suggest that the PV and LA-PV interfaces incorporate relatively independent, stable, and high-frequency AF drivers in this model.

Optical mapping of cardioversion of AF by MSE

The in vitro studies confirmed the DFT superiority of MSE compared with BPS. The atrial DFT of MSE observed in these studies ($n = 7$) was 3.88 ± 0.9 V/cm (1.2 ± 0.2 J) versus 9.40 ± 1.34 V/cm (3.4 ± 0.4 J) for BPS ($p < 0.05$). To illustrate a possible mechanism of successfully decreasing the DFT with MSE, we took a 2-fold approach. First, we analyzed the spatial sequence of activation after each stage of a representative, successfully delivered MSE trial (Fig. 4). The spatial evolution of the tissue response after the application of MSE was then contrasted between an example of successful MSE application (with a peak voltage of 7 V/cm in this case) and an unsuccessful application (5 V/cm) from the same animal (Fig. 5).

During this example of an AF episode, 2 initiating localized foci were noted, the first coming from the left superior PV (Fig. 4A) and another from the right superior PV (Fig. 4B). Figure 4C shows the activation pattern when Stage 1 shocks were delivered, causing fast activation of the LA in ~60 ms, compared with ~90 ms during AF. The first shock of Stage 2 was delivered during the atrial refractory period and thus failed to initiate a new action potential. The remaining 5 Stage 2 shocks (Figs. 4D to 4H) activated the LA in a left-to-right activation pattern. Successive Stage 2 shocks resulted in increasingly regularized activation patterns (compare Fig. 4D with Fig. 4H). Finally, Stage 3 stimuli activated the atria in a pattern nearly identical to that seen during sinus rhythm, in which the wave front spread from the RA to the LA via Bachmann's bundle.

In Figure 5, each map charts the phase distribution immediately after each intervention in MSE. The top left panel shows a representative OAP with the color distribution of phase. Because AF is a complex, multidriver arrhythmia, the 2 shocks in Stage 1 must disrupt these drivers and spatially homogenize the potential. Because this process is both time- and peak voltage–sensitive, having 2 shocks increases the likelihood of successfully targeting the optimal delivery time. Both shocks combine to incrementally homogenize the tissue in Figure 5A, whereas in Figure 5B, the first shock fails and the second leaves some regions in various phases. In the successful case, Stage 2 shocks then sequentially capture more of the tissue, restraining the source of the arrhythmia from recurring. Stage 3 can clearly drive the whole tissue in the successful case and prime the tissue for sinus rhythm, which resumes ~700 ms after the last application of MSE Stage 3. Stage 2 fails in the unsuccessful case; as a result, the focal drivers of the arrhythmia reemerge before the end of Stage 2. Therefore, MSE succeeds at a lower peak voltage because Stage 1 can reset the tissue, which allows the Stage 2 shocks to slowly increase the amount of tissue that is captured by the applied shocks, preventing any critical points that may result from the virtual electrode polarization (VEP) of the initial shocks or the original drivers to reinitiate the arrhythmia. This action thus prepares the atria for the pacing spikes of Stage 3 to reset the repolarization pathway.

Discussion

Our results show that MSE significantly reduced the DFT compared with BPS in an in vivo canine model of tachypacing-induced, self-sustaining AF and in vitro atrial preparations. In vivo, MSE significantly reduced the total energy (0.16 ± 0.16 J vs. 1.48 ± 0.91 J) and the peak shock voltage (31.1 ± 19.3 V vs. 165 ± 34 V) compared with BPS.

Electrocardiographic analysis of defibrillation in vivo is limited by low spatial resolution and saturation of the electrogram during the application of shocks. Therefore, we investigated the biophysical mechanism of cardioversion by MSE using optical imaging in vitro, which is immune to shock-induced artifacts (21). The optical imaging studies found that MSE gradually eliminated the foci localized around the PV-LA interfaces that sustain AF until sinus rhythm was restored, as previously observed in therapy of ventricular tachycardia (15).

Chronic high-rate atrial pacing model of AF

This study used an animal model in which chronic atrial tachypacing induces structural and electrical remodeling similar to that observed in humans with AF (22-28). The similarities suggest that this is a plausible model in which to study cardioversion of AF, and they increase the likelihood that the differences in atrial DFT between standard BPS and experimental MSE observed in this canine model will extend to humans (29,30). The degree of remodeling was not characterized in this experiment, and variability may exist between individual animals.

Termination mechanism

The high-resolution analysis of defibrillation during AF showed that MSE, over the course of the multiple shock and pacing therapies, gradually eliminates these localized foci until sinus rhythm is restored. In past experiments on AF defibrillation, we relied on the secondary sources of excitation caused by the virtual electrodes of higher-voltage shocks to self-direct the restoration of sinus rhythm (12). However, in the case of MSE, the Stage 2 shocks play this role after the Stage 1 shocks, sequentially advancing more of the tissue and allowing the Stage 3 pacing to reset the rhythm for the restoration of sinus beats. This actively-controlled therapy allows for the successful decrease in both peak voltage and total energy, and it can be delivered from intravenously-deployed leads placed in commonly used implantation sites (RA and CS).

Study limitations

The mechanistic conclusions drawn from this study are limited to the interpretation of observed potential and phase responses in several preparations and are not extended to a quantified description. In addition, the optical mapping results are limited by the fact that the intact heart was dissected to image the endocardial surface of the LA and PVs. It is possible that this process may have disrupted the localized circuits of the intrinsic in vivo arrhythmia. Also, during the in vitro studies, the energy was delivered uniformly across the atria from 2 large electrodes on the exterior of the tissue. This method is different from the electrode orientation used during the in vivo studies. Despite these limitations, MSE significantly lowered the atrial DFT both in vitro and in vivo compared with BPS. Future studies will be performed to evaluate the probability of success of the MSE treatment at the lower voltages and to determine efficacy. This investigation provides valuable insight into the biophysical response to, and mechanism of, MSE to restore sinus rhythm, and it demonstrates that MSE achieved significantly lower atrial DFTs than the existing clinical standard (i.e., BPS).

Toward pain-free cardioversion of AF

Using BPS, delivered from a transvenous atrial lead system similar to that described in the present report, Lok et al. (6) found that nonsedated patients in AF for >1 month tolerated shocks of 2.5 ± 1.3 J, whereas Murgatroyd and Camm (31) reported that patients required sedation for shocks >1.1 to 1.2 J. Importantly, the mean DFT of MSE in the canine model of tachypacing-induced AF used in our study was 0.16 J. Using a chronically-implanted device, Wellens et al. (32) reported that a 2.5- to 2.7-J biphasic shock delivered from leads implanted in the RA and CS terminated 86.3% of AF episodes. Thus, although future studies

in humans will be necessary, it is likely that the use of MSE in an implantable, transvenous lead–based device will be significantly superior to previous devices that relied on BPS. If VSET is found to be higher in humans, the energy of Stage 2 could be optimized at lower levels than 60% VSET.

Conclusions

This study used a rapid atrial pacing model of AF to measure the atrial DFT of a standard BPS compared with MSE for potential use in an implantable device–based atrial cardioverter. In vitro optical imaging studies indicated that AF in this canine model was maintained by multiple, rapidly firing localized foci at the PV-LA interface. MSE gradually eliminated these foci by using a sequence of shocks followed by pacing. In vivo, MSE terminated AF with significantly lower energy and voltage compared with BPS. The mean atrial DFT of MSE in this study was below the shock strength that has been reported to cause pain in humans during in vivo testing, suggesting that device-based, pain-free atrial defibrillation may be achievable.

Acknowledgments

The authors thank Phillip S. Cuculich, MD, Timo Weimar, MD, Yoshiyuki Watanabe, MD, Toshinobu Kazui, MD, Diane Toeniskoetter, Naomi Still, Mitchell N. Faddis, MD, PhD, and Daniel H. Cooper, MD, for technical assistance and help in preparing the manuscript.

This study was supported by grants from the National Institutes of Health (R01HL067322, R01HL115415, and T32HL007081) and by Cardialen. Dr. Li is a former employee of Cardialen and is now an employee of St. Jude Medical. Dr. Schuessler received a research grant from and has served as a consultant for Cardialen. Dr. Efimov is a cofounder, shareholder, member of the board of directors, and chairman of the scientific advisory board of Cardialen; is a consultant to Phillips Healthcare; and has received grant support from the National Institutes of Health. All other authors have reported that they have no relationships relevant to the contents of this paper to disclose.

References

1. Miyasaka Y, Barnes ME, Gersh BJ, et al. Secular trends in incidence of atrial fibrillation in Olmsted County, Minnesota, 1980 to 2000, and implications on the projections for future prevalence. Circulation. 2006; 114:119–25. [PubMed: 16818816]
2. Weerasooriya R, Khairy P, Litalien J, et al. Catheter ablation for atrial fibrillation: are results maintained at 5 years of follow-up? J Am Coll Cardiol. 2011; 57:160–6. [PubMed: 21211687]
3. Lee WC, Lamas GA, Balu S, Spalding J, Wang Q, Pashos CL. Direct treatment cost of atrial fibrillation in the elderly American population: a Medicare perspective. J Med Econ. 2008; 11:281–98. [PubMed: 19450086]
4. Schmitt C, Alt E, Plewan A, et al. Low energy intracardiac cardioversion after failed conventional external cardioversion of atrial fibrillation. J Am Coll Cardiol. 1996; 28:994–9. [PubMed: 8837580]
5. Ladwig KH, Marten-Mittag B, Lehmann G, Gundel H, Simon H, Alt E. Absence of an impact of emotional distress on the perception of intracardiac shock discharges. Int J Behav Med. 2003; 10:56–65. [PubMed: 12581948]
6. Lok NS, Lau CP, Tse HF, Ayers GM. Clinical shock tolerability and effect of different right atrial electrode locations on efficacy of low energy human transvenous atrial defibrillation using an implantable lead system. J Am Coll Cardiol. 1997; 30:1324–30. [PubMed: 9350935]
7. Weigner MJ, Caulfield TA, Danias PG, Silverman DI, Manning WJ. Risk for clinical thromboembolism associated with conversion to sinus rhythm in patients with atrial fibrillation lasting less than 48 hours. Ann Intern Med. 1997; 126:615–20. [PubMed: 9103128]

8. Steinhaus DM, Cardinal DS, Mongeon L, Musley SK, Foley L, Corrigan S. Internal defibrillation: pain perception of low energy shocks. Pacing Clin Electrophysiol. 2002; 25:1090–3. [PubMed: 12164452]
9. Mitchell AR, Spurrell PA, Gerritse BE, Sulke N. Improving the acceptability of the atrial defibrillator for the treatment of persistent atrial fibrillation: the atrial defibrillator sedation assessment study (ADSAS). Int J Cardiol. 2004; 96:141–5. [PubMed: 15262026]
10. Geller JC, Reek S, Timmermans C, et al. Treatment of atrial fibrillation with an implantable atrial defibrillator—long term results. Eur Heart J. 2003; 24:2083–9. [PubMed: 14643268]
11. Daoud EG, Timmermans C, Fellows C, et al. for the Metrix Investigators. Initial clinical experience with ambulatory use of an implantable atrial defibrillator for conversion of atrial fibrillation. Circulation. 2000; 102:1407–13. [PubMed: 10993860]
12. Ambrosi CM, Ripplinger CM, Efimov IR, Fedorov VV. Termination of sustained atrial flutter and fibrillation using low-voltage multiple-shock therapy. Heart Rhythm. 2011; 8:101–8. [PubMed: 20969974]
13. Li L, Nikolski V, Wallick DW, Efimov IR, Cheng Y. Mechanisms of enhanced shock-induced arrhythmogenesis in the rabbit heart with healed myocardial infarction. Am J Physiol Heart Circ Physiol. 2005; 289:H1054–68. [PubMed: 15879480]
14. Ripplinger CM, Krinsky VI, Nikolski VP, Efimov IR. Mechanisms of unpinning and termination of ventricular tachycardia. Am J Physiol Heart Circ Physiol. 2006; 291:H184–92. [PubMed: 16501014]
15. Li W, Ripplinger CM, Lou Q, Efimov IR. Multiple monophasic shocks improve electrotherapy of ventricular tachycardia in a rabbit model of chronic infarction. Heart Rhythm. 2009; 6:1020–7. [PubMed: 19560090]
16. Li W, Janardhan AH, Fedorov VV, Sha Q, Schuessler RB, Efimov IR. Low-energy multistage atrial defibrillation therapy terminates atrial fibrillation with less energy than a single shock. Circ Arrhythm Electrophysiol. 2011; 4:917–25. [PubMed: 21980076]
17. Janardhan AH, Li W, Fedorov VV, et al. A novel low-energy electrotherapy that terminates ventricular tachycardia with lower energy than a biphasic shock when antitachycardia pacing fails. J Am Coll Cardiol. 2012; 60:2393–8. [PubMed: 23141483]
18. Fedorov VV, Schuessler RB, Hemphill M, et al. Structural and functional evidence for discrete exit pathways that connect the canine sinoatrial node and atria. Circulation Res. 2009; 104:915–23. [PubMed: 19246679]
19. Kalifa J, Tanaka K, Zaitsev AV, et al. Mechanisms of wave fractionation at boundaries of high-frequency excitation in the posterior left atrium of the isolated sheep heart during atrial fibrillation. Circulation. 2006; 113:626–33. [PubMed: 16461834]
20. Laughner JI, Ng FS, Sulkin MS, Arthur RM, Efimov IR. Processing and analysis of cardiac optical mapping data obtained with potentiometric dyes. Am J Physiol Heart Circ Physiol. 2012; 303:H753–65. [PubMed: 22821993]
21. Efimov IR, Cheng Y, Van Wagoner DR, Mazgalev T, Tchou PJ. Virtual electrode-induced phase singularity: a basic mechanism of defibrillation failure. Circ Res. 1998; 82:918–25. [PubMed: 9576111]
22. Daoud EG, Bogun F, Goyal R, et al. Effect of atrial fibrillation on atrial refractoriness in humans. Circulation. 1996; 94:1600–6. [PubMed: 8840850]
23. Goette A, Honeycutt C, Langberg JJ. Electrical remodeling in atrial fibrillation. Time course and mechanisms. Circulation. 1996; 94:2968–74. [PubMed: 8941128]
24. Wijffels MC, Kirchhof CJ, Dorland R, Allessie MA. Atrial fibrillation begets atrial fibrillation. A study in awake chronically instrumented goats. Circulation. 1995; 92:1954–68. [PubMed: 7671380]
25. Fareh S, Villemaire C, Nattel S. Importance of refractoriness heterogeneity in the enhanced vulnerability to atrial fibrillation induction caused by tachycardia-induced atrial electrical remodeling. Circulation. 1998; 98:2202–9. [PubMed: 9815876]
26. Gaspo R, Bosch RF, Talajic M, Nattel S. Functional mechanisms underlying tachycardia-induced sustained atrial fibrillation in a chronic dog model. Circulation. 1997; 96:4027–35. [PubMed: 9403628]

27. Gaspo R, Bosch RF, Bou-Abboud E, Nattel S. Tachycardia-induced changes in Na+ current in a chronic dog model of atrial fibrillation. Circulation Res. 1997; 81:1045–52. [PubMed: 9400386]
28. Yue L, Feng J, Gaspo R, Li GR, Wang Z, Nattel S. Ionic remodeling underlying action potential changes in a canine model of atrial fibrillation. Circulation Res. 1997; 81:512–25. [PubMed: 9314832]
29. Mandapati R, Skanes A, Chen J, Berenfeld O, Jalife J. Stable microreentrant sources as a mechanism of atrial fibrillation in the isolated sheep heart. Circulation. 2000; 101:194–9. [PubMed: 10637208]
30. Skanes AC, Gray RA, Zuur CL, Jalife J. Effects of postshock atrial pacing on atrial defibrillation outcome in the isolated sheep heart. Circulation. 1998; 98:64–72. [PubMed: 9665062]
31. Murgatroyd FD, Camm AJ. Atrial fibrillation: the last challenge in interventional electrophysiology. Br Heart J. 1995; 74:209–11. [PubMed: 7547010]
32. Wellens HJ, Lau CP, Luderitz B, et al. Atrioverter: an implantable device for the treatment of atrial fibrillation. Circulation. 1998; 98:1651–6. [PubMed: 9778331]

Abbreviations and Acronyms

ASET	atrial shock excitation threshold
BPS	single biphasic shock
CS	coronary sinus
DFT	defibrillation threshold
HRP	high-rate pacing
LA	left atrium
LPA	left pulmonary artery
MSE	multistage electrotherapy
OAP	optical action potential
PV	pulmonary vein
RA	right atrium
RAA	right atrial appendage
VSET	ventricular shock excitation threshold

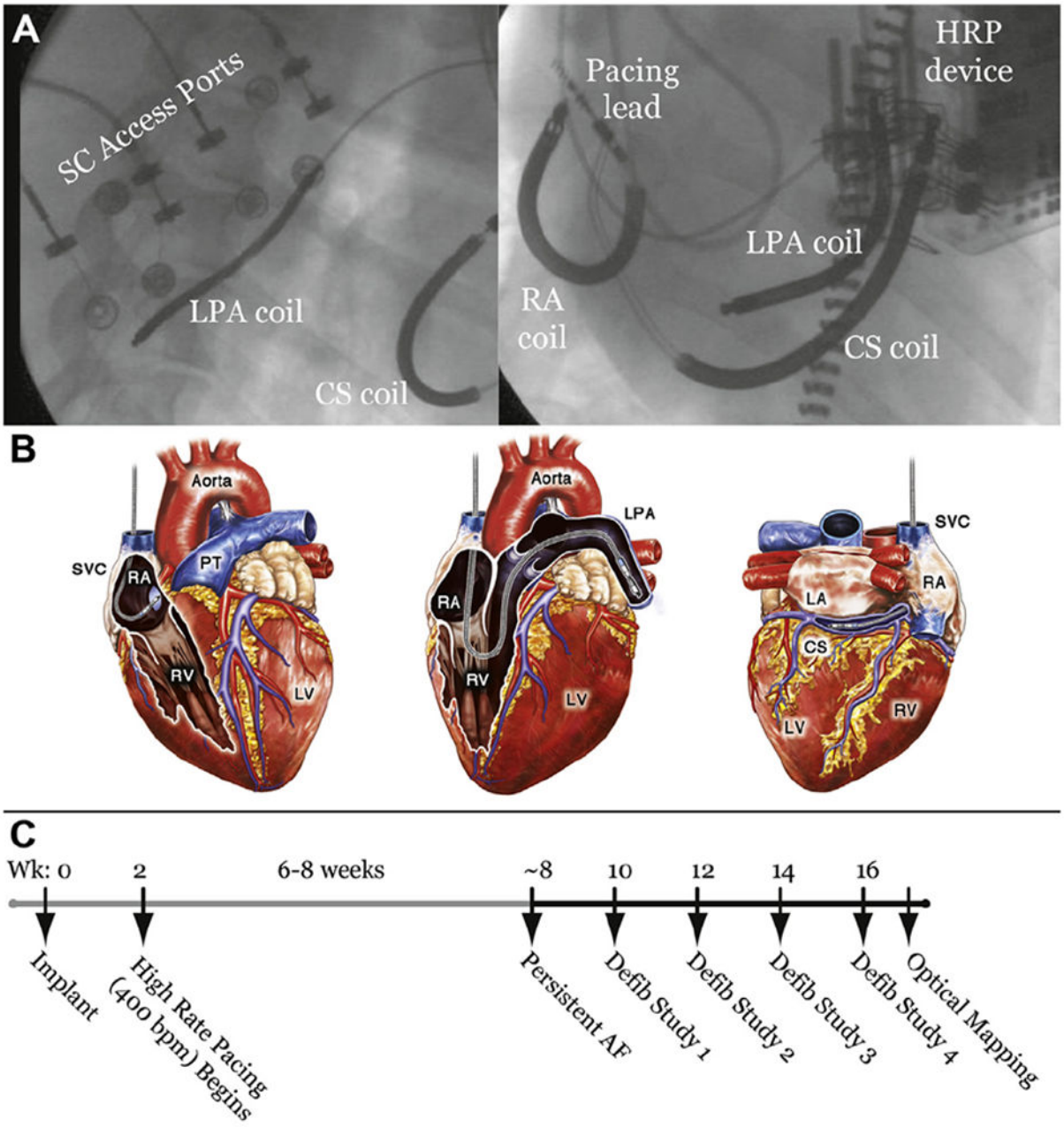

Figure 1. Chronically Implanted Lead Positions and Experimental Timeline

(A) Fluoroscopic images of the anatomic positions of chronically-implanted transvenous leads and subcutaneous (SC) access ports from left lateral **(left panel)** and left anterior oblique **(right panel)** views. **(B)** Schematic depiction of lead positions. Shocks were delivered from the right atrium (RA) coil to the left pulmonary artery (LPA) coil or the RA coil to the coronary sinus (CS) coil. **(C)** Experimental timeline showing model development and approximate times of defibrillation (defib) studies. AF = atrial fibrillation; HRP = high rate pacing; LA = left atrium; LV = left ventricle; PT = pulmonary trunk; RV = right ventricle; SVC = superior vena cava; Wk = week.

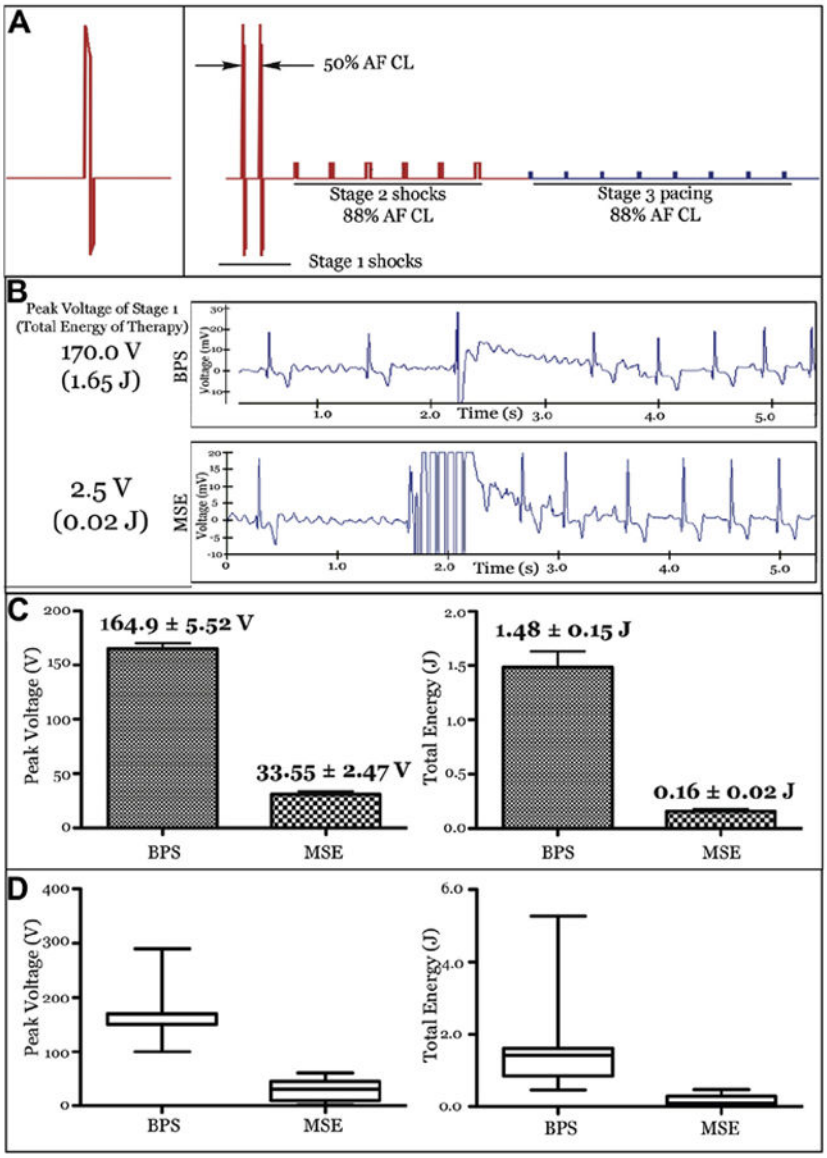

Figure 2. In Vivo Cardioversion of AF by BPS Versus MSE

(A) Defibrillation therapies tested. The **left panel** shows a single truncated exponential single biphasic shock (BPS). The **right panel** shows the multistage electrotherapy (MSE). Therapy in **red** was delivered through defibrillation coils, whereas the **blue** stage was delivered through the right atrial appendage pacing lead. **(B)** Surface electrogram and defibrillation threshold (DFT) of the sample in vivo atrial fibrillation (AF) terminations by using BPS and MSE. (**C** and **D**) Summary of in vivo atrial DFTs (n = 8) for BPS versus MSE. The peak shock voltage represents the maximum leading-edge voltage required for cardioversion by BPS or BPS delivered in Stage 1 of MSE. The total energy represents the sum of the energy of all stages of each therapy. Values are mean ± SE in **C** and median + quartiles in **D**.

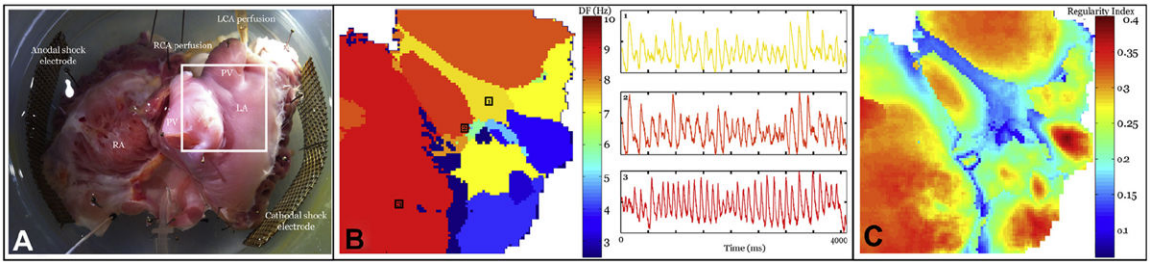

Figure 3. DF Analysis of AF In Vitro

(A) In vitro tissue preparation of the endocardial canine atrium used to record optical action potentials (OAPs). Field of view is shown by the **white box**. **(B)** Spatial map of the dominant frequency (DF) during the sample in vitro AF episode. Example OAP traces during AF are shown from the selected regions. **(C)** Spatial pattern of regularity index. A value close to 1 represents a highly stable region with a narrow power distribution around DF. Regions close to the pulmonary veins (PVs) show increased stability compared with the free atrial wall. LCA = left coronary artery; RCA = right coronary artery; other abbreviations as in Figure 1.

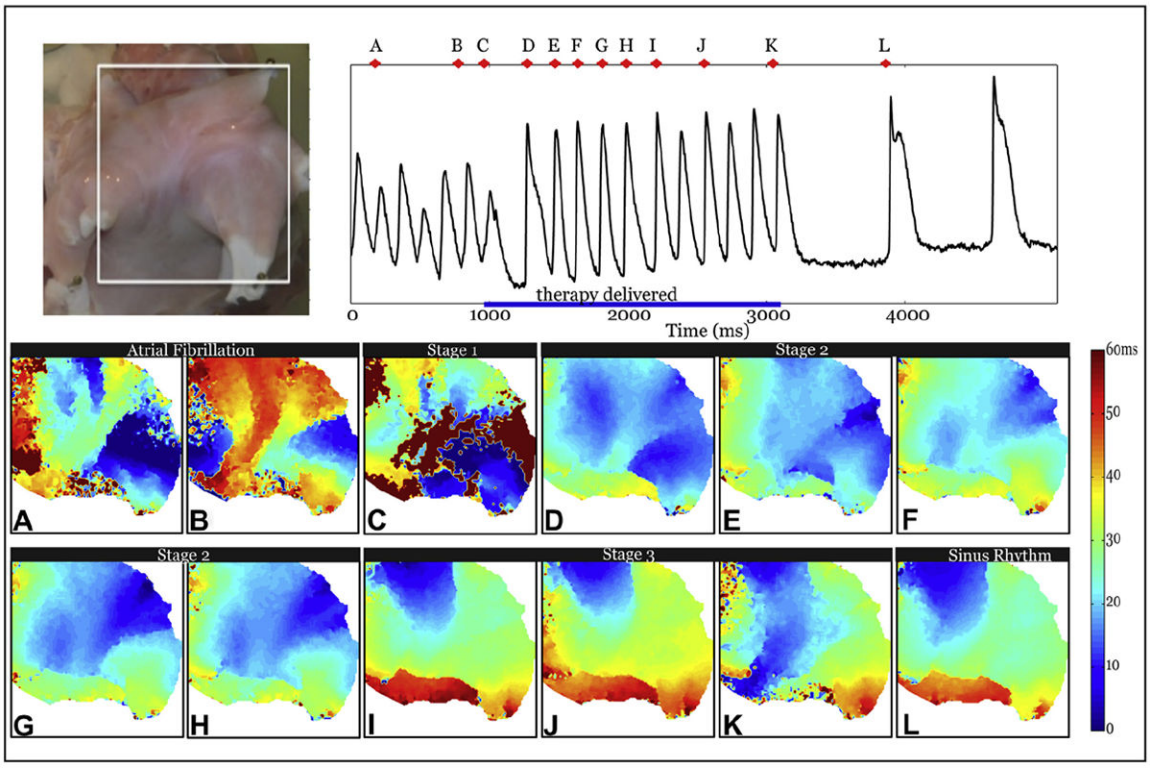

Figure 4. Optical Mapping of Successful Termination of AF by MSE

The **white box in the top left panel** shows the field of view. Activation maps during a representative successful application of MSE with a peak voltage of 7 V/cm. (**A** and **B**) AF **(C)** Stage 1 shocks. (**D** to **H**) Stage 2 shocks. (**I** to **K**) select Stage 3 pulses. **(L)** Restored sinus rhythm. Abbreviations as in Figure 2.

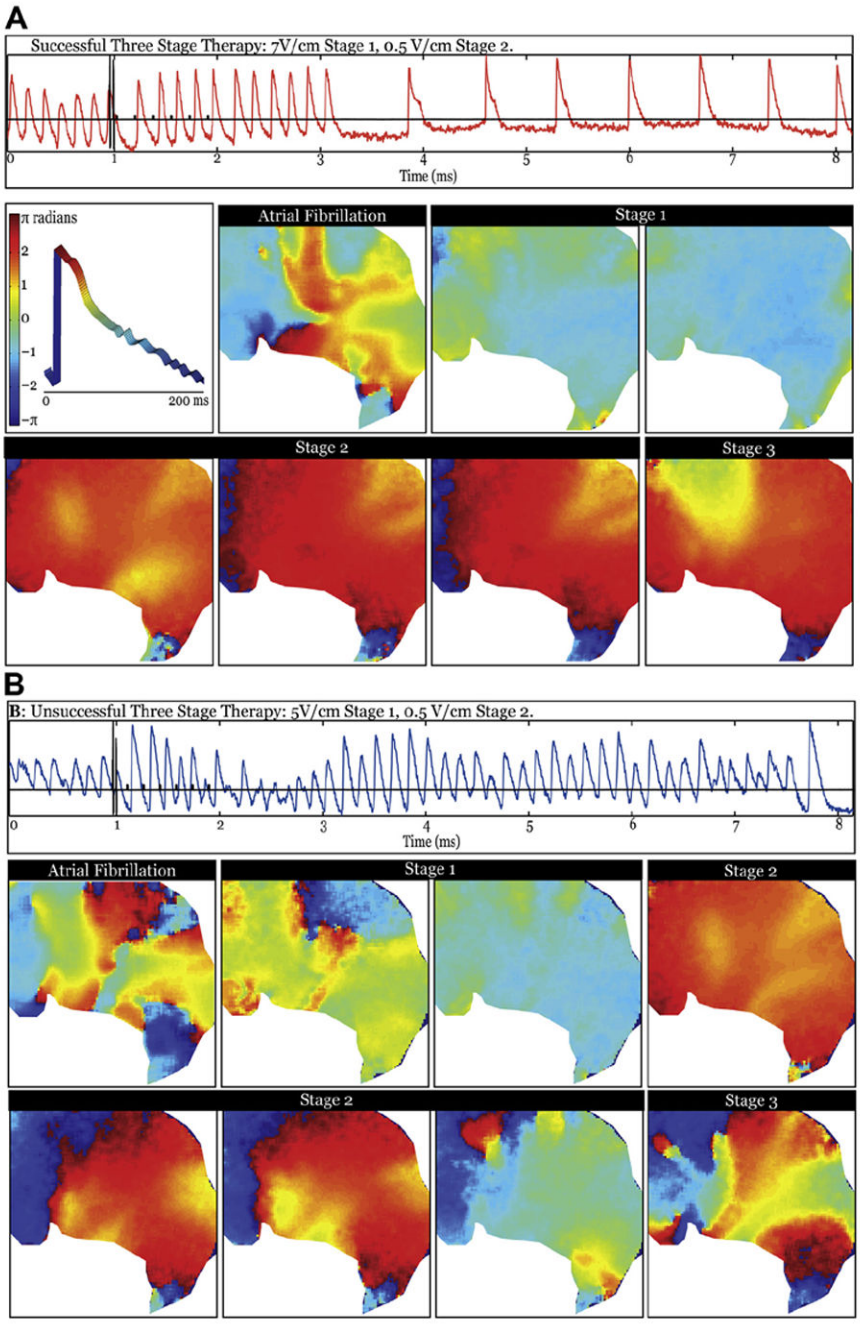

Figure 5. Phase Analysis of Successful and Unsuccessful Termination of AF by MSE

Spatial maps of phase immediately after each intervention of MSE in sample successful and unsuccessful terminations. **(A)** Successful termination with a peak shock strength of 7 V/cm displayed with representative optical trace from middle of the field of view **(orange trace)**. The panels show the evolution of phase during therapy application, beginning with an AF example, then proceeding to Stage 1 shocks 1 and 2; Stage 2 shocks 2, 4, and 6; and first stimulus of Stage 3. The **middle left panel in A** shows a representative optical action potential with the definition of phase. **(B)** Unsuccessful termination with a peak shock

strength of 5 V/cm displayed with representative optical trace from the middle of the field of view **(blue trace)**. Panels show evolution of failed response to therapy, starting from an AF example, then progressing to Stage 1 shocks 1 and 2; Stage 2 shocks 2 and 4 through 6; and first stimulus of Stage 3. Abbreviations as in Figure 2.